

Project Title:**Numerical studies on topological superconducting phases and Majorana zero modes in iron-based superconductors****Name: Qing Xie****Laboratory at RIKEN: Quantum Computational Science Research Team, RIKEN Center for Quantum Computing**

1. Background and purpose of the project, relationship of the project with other projects

Adiabatic control over quantum states is of fundamental importance for quantum information processing, quantum computation, and many other dynamic quantum processes. Nevertheless, adiabaticity can only be achieved in sufficiently slow processes, which inevitably expose the system to dissipation and noise. This presents a major obstacle and hinders many practical applications, such as quantum gate preparation and gate operations. Therefore, for the past few years, there have been intensive efforts aiming for protocols that speed up the evolution process and at the same time render the desired system within the adiabatic regime. These protocols are collectively called shortcuts to adiabaticity (STA).

Counterdiabatic (CD) driving is a powerful STA. It supplements an auxiliary time-dependent CD term to the original unassisted (UA) Hamiltonian, which suppress transitions among states and render the driving process transitionless. The CD term takes the form

$$C(t) = -i \sum_{m,n (m \neq n)} \frac{|m\rangle \langle m | \partial_t H | n \rangle \langle n |}{\epsilon_m - \epsilon_n},$$

where H is the UA model and $|m\rangle$ is the instantaneous eigenstate of H with eigenenergy ϵ_m . This expression exposes its limitations in two aspects: (i) it is not well-defined when a level crossing occurs at, e.g., a phase transition, as the spectrum gap closes at the crossing point. (ii) It is difficult to

implement since it requires precise control of the full spectrum over the driving period.

Recently, Claeys et al. [Phys. Rev. Lett. 123, 090602 (2019)] have proposed an approximate CD protocol which adopts a summation of 1 nested commutators to mimic the exact CD term. The adiabatic gauge potential takes the form

$$A_\lambda^{(l)}(t) = i \sum_{k=1}^l \alpha_k(t) O_{2k-1}(t),$$

with $O_k(t) = [H(t), O_{k-1}(t)]$ and $O_0 = \partial_\lambda H$. Here $\alpha_k(t)$ are real parameters that can be determined through minimize the action $S_l = \langle G_l, G_l \rangle_F$ with $G_l = \partial_\lambda H - i[H, A_\lambda^{(l)}]$. This approximate CD protocol has been applied to spin systems including the Ising and p-spin models.

Although be construction, this variational CD protocol is suitable for many-body fermionic systems, little effort has been devoted into this direction thus far. In this study, we apply this variational CD protocol proposed to a two-component fermionic Hubbard model in one spatial dimension.

2. Specific usage status of the system and calculation method

For the many-body systems, we employ the exact diagonalization method for the low-energy spectrum and Chebyshev polynomial expansion method for the time evolution. We present a Fortran package at

<https://github.com/QX20211202/HubbardCD>.

We have used 379,091 CPU hours in total.

3. Result

We study the time-dependent fermionic Hubbard model on a 1D chain consisting of L sites under open boundary conditions:

$$H(t) = H[\lambda(t)] = H_J + \lambda(t)H_U,$$

with

$$H_J = -J \sum_{\langle i,j \rangle, \sigma} c_{i\sigma}^\dagger c_{j\sigma} + \text{H.c.}$$

and

$$H_U = U \sum_i n_{i\uparrow} n_{i\downarrow}.$$

The driving function is chosen as

$$\lambda(t) = \sin^2 \left[\frac{\pi}{2} \sin^2 \left(\frac{\pi t}{2T} \right) \right].$$

Our primary concern is the time evolution of fidelities $F_{tt} = |\langle n(t) | \psi(t) \rangle|^2$, $F_{0t} = |\langle n(0) | \psi(t) \rangle|^2$, $F_{Tt} = |\langle n(T) | \psi(t) \rangle|^2$, where $n(t)$ is the instantaneous ground state of the UA model, and $\psi(t)$ is the time-evolved state driven by either the UA or CD models.

Figure 1 shows the time evolution of fidelity F_{tt} with respect to the scaled time $\tau = t/T$ for the UA and CD models with $U = 8$ and different system sizes $L = 8, 10, 12$, and 14 . It is clear from the figure that, for each system size, increasing the driving order l remarkably improves the fidelity during the evolution.

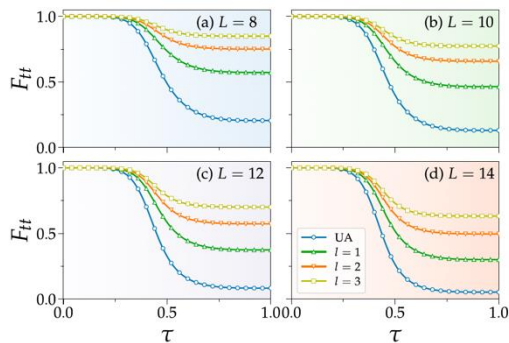


Fig. 1. The time evolution of fidelity F_{tt} for the UA model and the CD models with different driving orders $l = 1, 2, 3$ on the 1D chains of (a) $L = 8$, (b) $L = 10$, (c) $L = 12$ and (d) L

$= 14$ sites at half filling. The parameters are $U = 8$, $T = 0.1$, $NT = 100$, $\Delta T = 0.001$ and $N = 10$. Here time in the horizontal axis is scaled by the driving period T , i.e., $\tau = t/T$.

Figure 2 shows the time evolution of the three different fidelities F_{tt} , F_{0t} , and F_{Tt} for the UA and CD models on $L = 14$ sites. We observe that the driving period $T = 0.1$ is within the impulse regime where the driving period is too short for the system to respond. For smaller system size ($L = 6$), large driving order can always achieve perfect fidelity throughout the evolution [see Q. Xie, et al., [Phys. Rev. B 106, 155153 \(2022\)](https://doi.org/10.1103/PhysRevB.106.155153) for details.]

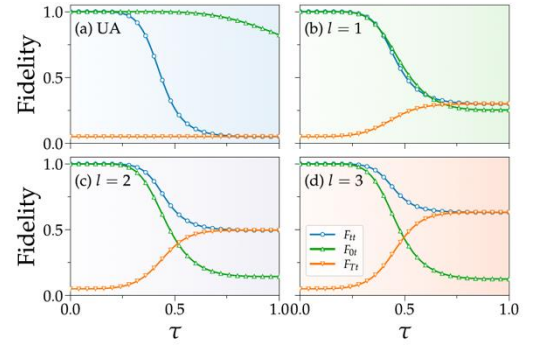


Fig. 2. The time evolution of fidelities F_{tt} , F_{0t} , and F_{Tt} for (a) the UA model and the CD models with (b) $l = 1$, (c) $l = 2$, and (d) $l = 3$ on the 1D chains of $L = 14$ sites at half filling. The remaining parameters are the same as in Fig. 1.

Figure 3 shows the evolution of fidelity F_{tt} for UA and CD models with $U = 8$ and $L = 14$ occupied by different number of fermions, $N_f = 6, 8, 10$, and 12 . We also observe higher fidelity with higher driving order l . However, we notice that for the 3rd driving order, the final fidelity for $N_f = 6$ and 12 are given by 79.09% and 83.94%, respectively, which means the $N_f = 12$ case has achieved better fidelity even though it has large Hilbert space. This suggests that the effectiveness of the CD driving depends non-monotonically on N_f and the Hilbert space dimension.

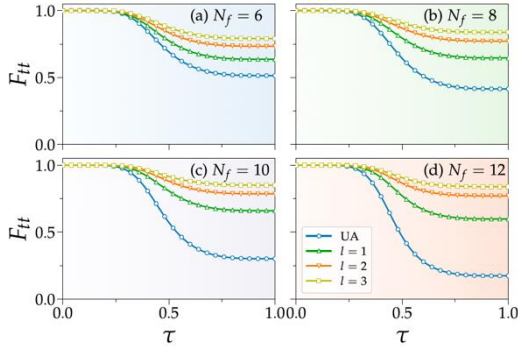


Fig. 3. The time evolution of fidelity F_{tt} for the UA model and the CD models with $l = 1, 2, 3$ on the 1D chains of $L = 14$ sites at different fermion fillings: (a) $N_f = 6$, (b) $N_f = 8$, (c) $N_f = 10$, and (d) $N_f = 12$. The results are obtained for the $S_z = 0$ sector. The remaining parameters are the same as in Fig. 1.

Figure 4 monitors the lowest two eigenvalues and the associated spectrum gap during the time evolution for $L = 8, 10, 12$, and 14 sites. In the UA model, the two eigenvalues monotonically increase with the evolution time, and the maxima of the gap appear at the beginning of the evolution. However, in the CD models, the spectra exhibit a valley-shaped structure, and the maxima of the gap appear around the middle of the time evolution.

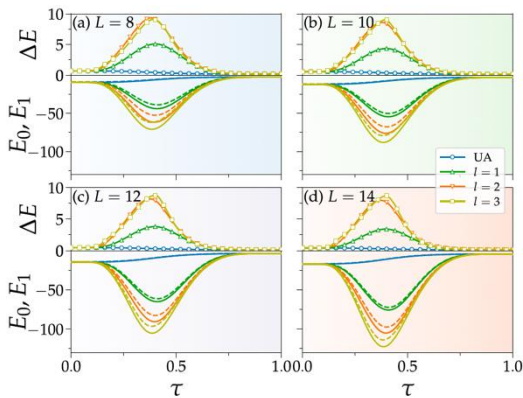


Fig. 4. The time evolution of the lowest two eigenvalues E_0 and E_1 , indicated by solid and dashed lines, respectively, in the lower panels and the corresponding spectrum gap in the upper panels for the UA and CD models on the 1D chain of (a) $L = 8$, (b) $L = 10$, (c) $L = 12$, and (d) $L = 14$ sites at half filling. The remaining parameters are the same as in Fig. 1.

In Figure 5, we study the T dependence of the final fidelity on $L = 12$ sites. We observe three regimes, i.e., an adiabatic regime for $T > T_{\text{adi}} \sim 10$, an impulse regime for $T < T_{\text{imp}} \sim 1.0$ and an intermediate regime inbetween. The adiabatic time can be estimated via the necessary condition for adiabaticity:

$$\sum_{m(\neq n)} \frac{|\langle m | \partial_t | n \rangle|}{\epsilon_m - \epsilon_n} \ll 1.$$

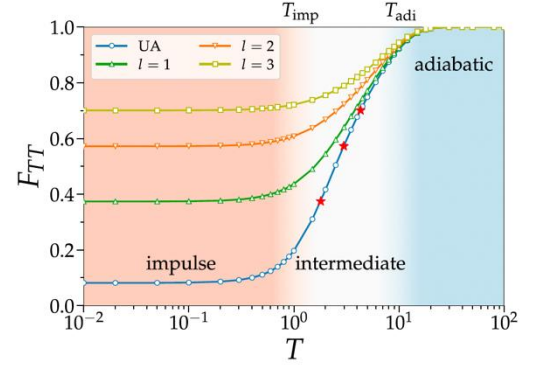


Fig. 5. The final fidelity F_{TT} as a function of the driving period T for the UA and CD models with $U = 8$ on $L = 12$ sites at half filling. For various T , the time step is fixed to be 0.001 . Three regimes, i.e., impulse, intermediate, and adiabatic regimes, distinguished by three colors crossover between themselves around T_{imp} and T_{adi} indicated at the top of the figure.

Figure 6 shows the final fidelity F_{TT} as a function of the interaction strength U for the UA and CD models on $L = 12$ sites. We observe two distinguish regimes: a weak-correlation regime for $U < U_c \sim 7$ and a strong-correlation regime for $U > U_c$. The CD protocol is more effective for the strong-correlation regime.

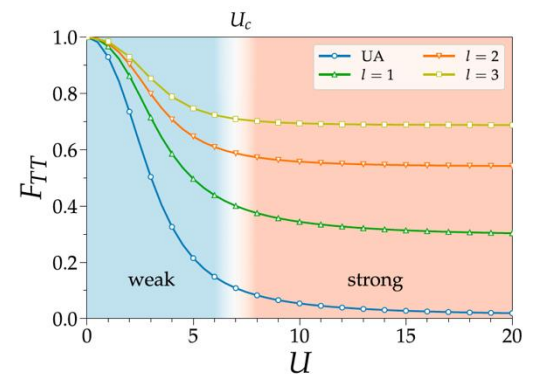


Fig. 6. The final fidelity F_{TT} as a function of the interaction

Usage Report for Fiscal Year 2022

strength U for the UA and CD models on $L = 12$ sites at half filling. Weak- and strong-correlation regimes crossover around U_c indicated at the top of the figure.

4. Conclusion

We have applied the variational CD driving protocol proposed by Claeys et al. to the 1D two-component fermionic Hubbard model. We have shown that the optimal variational parameters are the solution of a set of linear equations whose coefficients are given by the squared Frobenius norms of the nested commutators. We have devised an exact algorithm to construct analytical expressions of the nested commutators, which enables us to simulate systems up to $L = 14$ sites with the 3rd driving order. We have shown that the fidelity dramatically increases with increasing driving order throughout the evolution. Moreover, we have found that the CD driving protocol is more effective for the fast-driving regime with small driving period T and the strong-correlation regime with large interaction strength U , where the increase of the final fidelity is most significant when it is compared with the UA driving protocol. Our results demonstrate the usefulness of the variational CD protocol for interacting fermions and would be beneficial for further exploring fast ground-state preparation protocols for many-body fermion system on quantum computers in the foreseeable future.

5. Schedule and prospect for the future

We plan to study digital quantum simulation of the Hubbard model on NISQ hardware.

Usage Report for Fiscal Year 2022

Fiscal Year 2022 List of Publications Resulting from the Use of the supercomputer

[Paper accepted by a journal]

[1] Q. Xie, K. Seki, and S. Yunoki, Variational counterdiabatic driving of the Hubbard model for ground-state preparation, [Phys. Rev. B 106, 155153 \(2022\)](#).

[Conference Proceedings]

[Oral presentation]

[Poster presentation]

[Others (Book, Press release, etc.)]